

RESEARCH ARTICLE



Microwave-assisted Chitosan Based Activated Bentonite (CAB) for Cr (VI) Removal from Acid Mine Drainage

 OPEN ACCESS

Received: 13-01-2024

Accepted: 10-02-2024

Published: 29-05-2024

B V Thacker¹, G P Vadodaria^{2*}, G V Priyadarshi³, M H Trivedi³¹ Civil Engineering Branch, Gujarat Technological University, Ahmedabad, Gujarat, India² Principal, Government Engineering College, Bhavnagar, Gujarat, India³ Department of Earth and Environmental Science, KSKV Kachchh University, Bhuj-Kachchh, 370001, Gujarat, India

Citation: Thacker BV, Vadodaria GP, Priyadarshi GV, Trivedi MH (2024) Microwave-assisted Chitosan Based Activated Bentonite (CAB) for Cr (VI) Removal from Acid Mine Drainage. Indian Journal of Science and Technology 17(21): 2207-2217. <https://doi.org/10.17485/IJST/v17i21.94>

* Corresponding author.

gpv11@rediffmail.com

Funding: None

Competing Interests: None

Copyright: © 2024 Thacker et al. This is an open access article distributed under the terms of the [Creative Commons Attribution License](#), which permits unrestricted use, distribution, and reproduction in any medium, provided the original author and source are credited.

Published By Indian Society for Education and Environment ([iSee](#))

ISSN

Print: 0974-6846

Electronic: 0974-5645

Abstract

Background: Acid Mine Drainage (AMD) causes widespread environmental problems including the contamination of land and water bodies. The low-cost adsorbent synthesis from regional resources can be used for removal of toxic metals such as Cr (VI) from AMD. **Objectives:** Rapid synthesis of Chitosan based Activated Bentonite (CAB) nanocomposite adsorbent using microwave-assisted method for the removal of Cr (VI) from the acidic environment. **Methods:** The compositional and surface morphological characterization was conducted using FTIR, XRD, and FEG-SEM-EDS analysis. The Synthesized adsorbents were used to removal of Cr (VI) ion under different experimental conditions including initial concentration (45 to 120 mg L⁻¹), contact time (0 to 180 min), dose (0.25 to 4 g L⁻¹), solution pH (2 to 6). **Findings:** The optimum removal was 73.14 % at room temperature (27 °C), pH 2, concentration 90 mg L⁻¹ and 2.0 g L⁻¹ dose of CAB adsorbent. The field evaluation parameters such as ionic strength under various acids and regeneration ability show the potential applicability of the adsorbent in remediation of AMD. The kinetics models and adsorption isotherm were fitted with pseudo first order model (R² > 0.86) confirmed 49.62 mg g⁻¹ maximum adsorption capacity by Langmuir isotherm (R² > 0.93). **Novelty :** Novel microwave assisted rapid synthesis of CAB nanocomposites adsorbent has the possibility to use for large scale synthesis and elimination of Cr (VI) from the AMD.

Keywords: Chitosan; Activated bentonite; Cr (VI) removal; Adsorption isotherm; Kinetics rate models

1 Introduction

The Acid Mine Drainage (AMD) discharge from mining industries is one of the main causes for contamination of hydrosphere and lithosphere. Therefore, it becomes one of the concerning environmental challenges due to its highly acidic nature, other toxic metals and chemicals⁽¹⁾.

Chromium (Cr) is commonly found in Cr (III) and Cr (VI) in various industrial applications, including incineration facilities, cement, contaminated landfill, asbestos

lining erosion, tobacco smoke, topsoil, and rocks etc. The production of Chromite was 3,929 tonnes in India, while in the world 38,600 tonnes in the year of 2019-20⁽²⁾. The occurring mining waste might contain Cr (VI) are often, that leading to contamination of water bodies and land⁽³⁾. Cr (VI) is one of the highly toxic contaminates, which is found to be harmful to human health and life underwater. Exposure to high level of Cr (VI) can cause diarrhea, kidney failure, liver diseases, lung cancer, nausea, respiratory troubles and ulcer formation to the human body⁽⁴⁾. Therefore, the removal of Cr (VI) from the aqueous medium is still considering an interesting topic among the researchers. Many of them have recognised that adsorption is one of the cost effective, efficient, simple and reusable techniques among various conventional remediation processes^(1,5).

Chitosan, a biopolymer shows favourable characteristics for the absorption of heavy metal ions, primarily owing to the existence of amino groups (-NH₂) and hydroxyl (OH) functional groups within the structure. These amino groups engage with metal ions in the solution through processes involving ion exchange and complexation reactions.⁽⁶⁾ Similarly, in the last few years, clay minerals have attracted much interest because of their low cost, more active sites resulting into high pollutant removal efficiencies. Bentonite is a naturally abundant clay material known for its low conductivity, high cation exchange capacity, and substantial specific surface area. Silica (SiO₂), alumina (Al₂O₃), iron oxide (Fe₂O₃), magnesium oxide (MgO), calcium oxide (CaO), potassium oxide (K₂O), and sodium oxide (Na₂O) are the primary chemical components of bentonite⁽⁷⁾. Both are occurring naturally in the abundance; therefore, they have been used with modification as a low-cost adsorbent. Much work has been reported for the synthesis of chitosan-based Bentonite clay nanocomposites for the removal of contaminants from the water⁽⁸⁾. Recently, Bentonite-chitosan nanocomposite and beads were used to removal of Pb⁽⁹⁾ and Cr^(10,11) from the aqueous solution. They have used mechanical stirring method to synthesise chitosan based activated bentonite nanocomposite beads (CAB) which requires more than 4 hours stirring time. To reduce the time up to the 10 minutes for synthesis, the present study involves the microwave assisted synthesis of CAB nanocomposite.

Novel synthesized CAB nanocomposites beads were used removal to Cr (VI) ions from acidic environment. The present study involves the comprehensive characterization of CAB using FTIR, XRD, and FEG-SEM-EDS and pH_{ZPC} along with various parameters of adsorption of Cr (VI) like optimum dose, removal efficiency, equilibrium and kinetic for preparing adsorption isotherms. The field applicability of the adsorbent was evaluated using the ionic strength and regeneration & reusability for cost-effectiveness. The study shows potential applicability of the low cost adsorbent for removal of Cr (VI) ion form AMD.

2 Methodology

2.1 Activation of Raw Bentonite (RB)

Raw bentonite (RB) commercial grade sample was randomly collected from the Ashapura Perfoclay, Ltd, Bhuj, Gujarat. The collected RB sample was washed with deionized water (DIW) to remove the water-soluble inorganic components present in the RB sample. Afterward, the sample was dried in a hot air oven at 60°C for 5 hours to eliminate any moisture content. The RB was reacted with the 1 N HCL solution under the microwave irradiation at 350 W power and 2450 MHz for the (2×2) minutes⁽¹²⁾. The activated Bentonite (AB) was washed with DIW to obtain neutral pH 7. The AB sample was dried as mentioned above for RB and stored in a plastic container till further use for characterization and Application.

2.2 Microwave-assisted synthesis of Chitosan Activated Bentonite (CAB)

The microwave-assisted synthesis of chitosan-based composites was synthesized as per our previously reported⁽¹³⁻¹⁵⁾ work. The chitosan solution was prepared (using 1% acetic acid solution) by adding 1 ml glacial acetic acid (GAA) into DIW and making up to 100 ml. Then 1.8 g of commercial chitosan powder (purchased from PR chemicals, Himatnagar, Gujarat) was added into 80 ml solution. Simultaneously, 0.2 g activated Bentonite was added into 20 ml solution. Both the solutions were mixed in a 250 ml beaker and allowed sonication for 5 minutes while stirring. The reaction mixture was irradiated with microwave oven (LG model no.: MB-394AA) for (5×2) min at 350 W power and 2450 Mhz. Afterward the homogenized bobble free viscous gel-like solution was added drop by drop into 1N NaOH solution to prepare a CAB hydrogel. The obtained CAB hydrogel beads were rinsed with DIW till the pH~7, dried in an oven at 60°C for 24 h.

2.3 Characterization of CAB

The functional groups identification of the raw and synthesized material CS, RB, CAB before as well as after Cr removal CAB-Cr was conducted by FT-IR spectra (Perkin Elmer spectrum 400) within the range of 400-4000 cm⁻¹. The X-Ray Diffraction (XRD) spectra of these samples were recorded between specific 2θ values (i.e., 5° to 80°) by powder XRD Bruker D8 Advance to comprehend the crystal structure of the materials. The morphological and compositional characterization of CAB before and

after Cr removal CAB-Cr was performed using SEM (JEOL JSM-7600F) and EDS analysis, respectively. The Point Zero Charge (pH_{ZPC}) of synthesized adsorbent was estimated using the pH drifting method as per⁽¹⁶⁾.

2.4 Adsorption experiment for Cr (VI) removal

250 mg L⁻¹ standard stock solution of Cr (VI) was prepared by dissolving 141.40 mg K₂Cr₂O₇ in 200 ml of DIW. The working standards with different concentrations of Cr solution were obtained using dilution, and their concentrations were validated through a standard curve with an R² value of 0.98. The estimation of Cr (VI) was conducted using a UV-Visible spectrophotometer based di-phenylcarbazide method as per PCB manual. To evaluate the synthesized adsorbent (CAB) at the laboratory scale, an investigation was conducted to ascertain the influence of various parameters. These parameters included the initial Cr (VI) concentration, ranging from 45 to 120 mg/L, as well as the contact time, spanning from 0 to 180 minutes. Different parameters have been studied in the experimental set like different concentration, contact time, pH, dose and ionic strength. In a typical process, 50 mL volume of Cr (VI) solution with variable concentrations (45, 60, 90, 105 and 120 mg L⁻¹), pH (2,3, 4, 5, and 6) and dose (25, 50, 100 and 200 mg) have been taken. After achieving the results, samples were taken and analyzed using UV-visible spectrophotometer. The following well-known equations were applied to calculate the Cr (VI) removal efficiency (in percentage) and maximum Cr(VI) adsorption capacity of CAB (in mg g⁻¹).

$$Cr(VI) \text{ removal } \% = \frac{(\text{Initial } Cr(VI) \text{ concentration } (C_0) - \text{Final } Cr(VI) \text{ concentration } (C_e))}{\text{Initial } Cr(VI) \text{ concentration } (C_0)} \times 100\%$$

$$\text{Maximum } Cr(VI) \text{ sorption capacity } (q_e) = \frac{(C_0 - C_e) \times (\text{volume of } Cr(VI) \text{ solution } (v))}{(\text{dry weight } (W) \text{ of CAB})}$$

Where, C₀ and C_e are in mg/L, W is in gm and V is in L.

Adsorption kinetic experiments were performed with different Cr (VI) concentrations at pH 4 and room temperature. The obtained results were used to calculate the adsorption kinetic parameters using the pseudo-first order, pseudo-second order and intraparticle diffusion models. Langmuir, Freundlich and Temkin isotherm models were selected to examine the equilibrium results.

2.5 Evaluation of potential applicability of CAB towards simulated AMD

To identify the probable applicability of CAB towards the AMD treatment, the cost-benefit aspect (regeneration study), implication due to presence of various acidic anions (via ionic strength study).

2.5.1 Studies of salt solution implications on Cr (VI) removal efficiency

The presence of various ions and pollutants in acid drainage from mines, the influence of different ions at varying concentrations on the removal efficiency of Cr (VI) using CAB was investigated. In a standard reaction procedure, 100 mg of the adsorbent CAB were submerged in 50 mL of a Cr (VI) solution containing 90 mg L⁻¹ concentration at various pH depending upon pH of ionic solution. This solution contained individual acid solutions, including HCl, HNO₃, H₃PO₄, and H₂SO₄, each at concentrations of 1 and 25 mM. The mixture was agitated for 60 minutes.

2.5.2 Desorption and reusability studies of CAB towards Cr (VI)

To identify the regeneration capacity of the synthesized adsorbent CAB, the immediate adsorption and desorption process was performed in a batch mode. For which initially, 0.1 g of CAB was agitated with 50 mL of Cr (VI) solution having 90 mg L⁻¹ concentration for 180 min. Afterwards, the Cr (VI) saturated beads were separated by filtration process, dried in an oven (55-65 °C) for 12 hrs. These dried beads were desorbed, by agitating in 50 mL of NaOH solution (1N) for 60 min at 55 °C heating and stirring. Then after regenerated beads separated and dried for its second and subsequent adsorption-desorption cycles up to the five cycles. The recovered Cr (VI) using NaOH solution was measured using the same method as described above.

3 Results and Discussion

3.1 Characterization of the CS, RB, CAB and CAB-Cr

3.1.1 FTIR

Figure 1(a & b) represents the FT-IR spectra of CS and RB (a) and CAB before and after Cr removal (CAB-Cr) (b). The IR spectrum of CS in Figure 1(a) shows absorption peaks appear at 3558, 3478, and 3234 cm^{-1} , corresponding to the stretching vibrations of -OH groups and -NH₂, as well as the stretching vibrations of -CH₃ at 2926 cm^{-1} . Additionally, peaks at 1623 and 1378 cm^{-1} are attributed to the bending and stretching vibrations of the -CONH₂ and Amide III (C-N) groups, respectively. A broad peak and stretching vibrations at 1096 and 631 cm^{-1} correspond to -CO (pyranose ring) and -C₂H₅NO (N-acetyl) groups, respectively⁽¹⁷⁾. Figure 1(a) reveals the spectrum of RB absorption bands in the 3557-3778 cm^{-1} range, which can be attributed to Si-OH and Al-OH tensile vibrations⁽¹²⁾. Additionally, the spectrum shows peaks at 1638, 1048, 801, and 474 cm^{-1} , representing the absorption peaks of water angular deformations, symmetric Si-O-Si bond stretching and quartz vibration, Si-O-Si bending vibrations, respectively. Stretching vibrations at 3425 and 622 cm^{-1} indicate the presence of -OH groups within the interlayer and adsorbed water, as well as silanol groups and M-O-Si vibrations (M = Al, Mg) in the RB sample⁽¹⁸⁾. Figure 1(b) shows spectrum of CAB at 3793, 3380 and 1323 which represent hydroxyl (-OH) groups and group of chitosan biopolymer present on the surface and N-H groups, respectively⁽⁹⁾. The bands at 1645 and 1380 cm^{-1} represent the amide I group and CH₃ deformation. It also shows bands at 1010 and 516 cm^{-1} which refers to symmetric Si-O-Si stretching vibration and Si-O-Al bending vibrations, respectively⁽¹⁸⁾. The adsorption peak of CAB-Cr at 3787 cm^{-1} shifted after Cr (VI) adsorption from 3793 cm^{-1} which indicates that the interaction between Cr metal ion and chitosan through -OH and -NH group which was further confirmed by decrease in % T from 93 to 90^(19,20). Another peak at 1650 cm^{-1} was sifted from the 1656 cm^{-1} after the Cr (VI) adsorption that corresponds to carboxylic group. Similarly, all the adsorption peaks were shifted and the % transmission have been increased in each of the spectra of CAB-Cr.

3.1.2 XRD

Figure 1(c and d) represent the XRD spectra from 5 to 80° 2 θ value of various samples CS and RB (c) and CAB before & after Cr removal CAB-Cr (d). Figure 1(c) exhibits two distinct and prominent peaks of chitosan biopolymer at 2 θ values of 9.26 and 20.10 serve as compelling evidence that the crystal structure, predominantly existing in a hydrated form, has been confirmed⁽¹³⁾. The XRD analysis of the RB revealed the presence of sharp peak of Quartz at 2 θ value 28.73°, also the presence of distinct and sharp peaks corresponding to Montmorillonite at 2 θ value 21.92°, 30.75°, 37.65°, 45.38°, 52.27°, 63.72°. Figure 1(d) represents the corresponding peak of CAB for the CS and CAB both at 2 θ values with slightly shift to 9.71°, 20.85°, 29.55° and 39.63° respectively. After adsorption of Cr (VI) the XRD spectra shows no peak at 9.71° and reduction in peak at 19.89° which shows through adsorption it reduces the intramolecular crystallinity of CS⁽²⁰⁾. Similarly, the Quartz and montmorillonite peak at 2 θ values 26.66°, 30.24°, 35.70°, 57.38° and 62.96° etc. shows reduction after the adsorption of Cr (VI) in the CAB sample that confirmed the comparative amorphous surface to the CAB.

3.1.3 FEG-SEM-EDS

The size and shape of the synthesized CAB before & after Cr removal CAB-Cr was studied by analyzing the FEG-SEM images. The surface morphology and elemental composition of CAB and CAB-Cr samples are depicted in Figure 2(a & c) SEM images. The SEM image of CAB shows the nano (< 0.1 μm) pores on the surface, which may favour the transfer and adsorption of Cr (VI). After the adsorption a crystalline structure of Cr metal on the adsorbent surface can be confirmed by EDS spectra shown in the Figure 2(b & d), where the peak of Ca and Fe is dominated by the Cr due to adsorption on surface. Also, Table 1 represent elemental composition (weight %) of CAB before and after CAB-Cr, Where C; O and Cr were increased due to the adsorption of Cr₂O₇⁻² on the CAB, similar observation was found by⁽¹⁷⁾.

3.2 Cr (VI) removal experiment

The Cr (VI) removal efficiency of CAB was evaluated with various operating parameters and the obtained results are depicted in Figure 3(a-f).

3.2.1 Effect of initial Cr (VI) concentration with contact time

The results of effect of various concentrations 45, 60, 90, 105 and 120 mg L^{-1} of Cr (VI) solution on the removal percentage (% R) and maximum adsorption capacity (mg g^{-1}) efficiency of CAB adsorbent are shown in the Figure 3(a & b) respectively. Figure 3(a) illustrates a clear trend where, as the initial Cr (VI) concentration rises from 45 to 120 mg L^{-1} , the removal

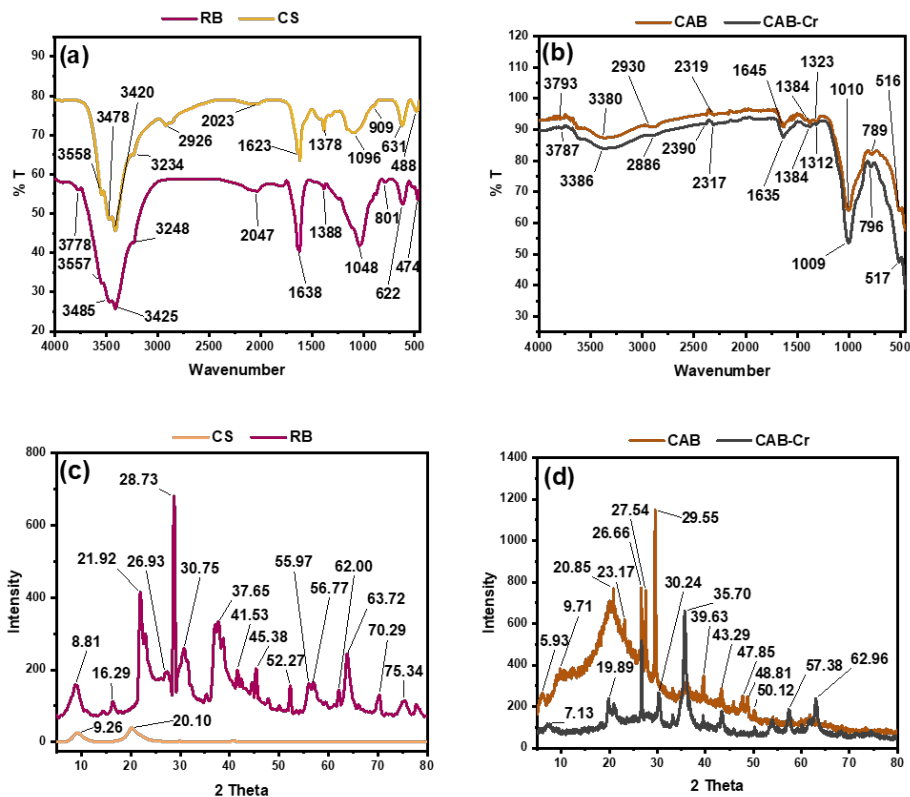


Fig 1. FT-IR of CS and RB (a), CAB before & after Cr removal CAB-Cr (b) and XRD spectra of CS and RB (c), CAB before & after Cr removal CAB-Cr (d)

Table 1. Elemental composition of CAB before and after Cr removal (CAB-Cr) using EDX analysis

Elemental Composition	CAB (wt %)	CAB-Cr (wt %)
Carbon	5.84	34.67
Oxygen	35.69	63.37
Silicon	4.75	0.25
Aluminium	2.64	1.09
Iron	50.07	0.0
Calcium	1	0.0
Chromium	0.0	0.62
Total	100 %	100 %

percentage correspondingly increases from 43.59 % to 61.92 %. This substantial increase in removal percentage at higher Cr (VI) concentrations is primarily attributed to the saturation of sorption sites on the surface of the beads. In the same scenario, as the concentration of Cr (VI) increased, the observed adsorption capacity (q_e) exhibited a significant rise, escalating from 9.8 to 37.15 mg g^{-1} . Same observations were found with SDS modified Chitosan nanocomposite⁽⁵⁾ by increasing concentration from 10 to 100 mg L^{-1} the adsorption capacity also increased 0.88 to 0.89 mg g^{-1} . The increase in adsorption can be attributed to the increased attraction of Cr (VI) molecules for the surface of the beads as their concentration rises. It has been previously noted that an increased concentration of Cr (VI) leads to a greater driving force for mass transfer^(10,21). The impact of varying contact duration, ranging from 0 to 180 minutes, on the adsorption of Cr (VI) by nanocomposite beads is illustrated in the accompanying figure. It is evident that during the initial 90 minutes of interaction between the adsorbent and the adsorbate, both the removal rate (%) and the maximum adsorption capacity (q_e) demonstrated concurrent increments alongside the Cr

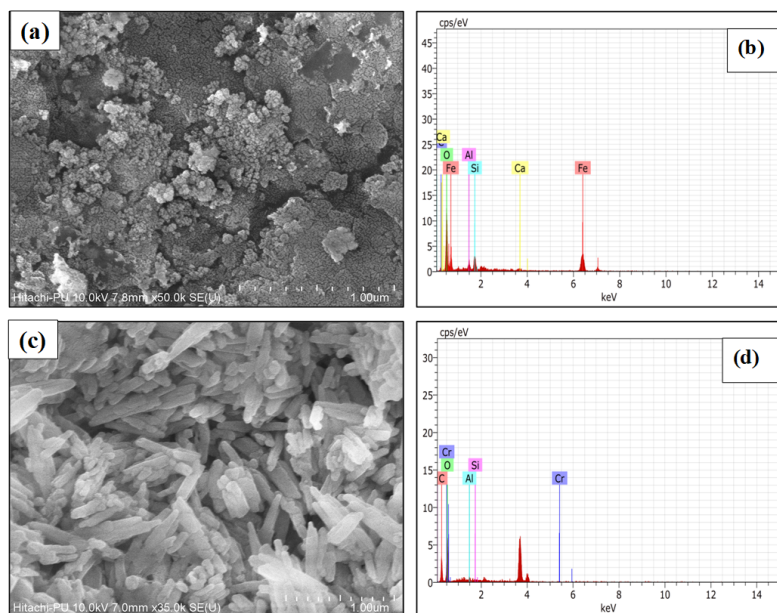


Fig 2. SEM microphotographs and EDS spectra of CAB before (a and b) & after Cr removal CAB-Cr (c and d)

(VI) concentrations.

3.2.2 Effect of solution pH

The pH of the working solution plays a significant role in influencing the adsorption process. It serves a dual function by regulating both the active surface charges on the CAB and the solubility and ionization of Cr (VI) molecules within the solution/effluent⁽²²⁾. Hence, it is essential to optimize the pH conditions for the application of the adsorbent. In this context, a study was conducted to determine the ideal pH for the removal of Cr (VI) utilizing CAB, with a focus on acidic pH values including 2, 3, 4, 5 and 6. Figure 3 (c), The obtained experimental results have shown a consistency with previous studies^(10,11) that the increasing pH from 2 to 6 in the solution led to decrease in Cr (VI) removal percentage from 73.14 to 22.3 % R. The higher removal of Cr (VI) in acidic pH is due to the tenacious electrostatic attraction between positively charged functional groups (i.e., silanol groups Si-OH, Al³⁺ and R₃NH⁺) on the surface of adsorbent (CAB with pH_{ZPC} = 7.9). The removal efficiency of Cr (VI) remained relatively consistent in the range of pH 3.0 and 5.0. Furthermore, near to pH 6 it shows the lowest removal for the Cr (VI) ion from the solution.

3.2.3 Effect of CAB dose

The synthesized CAB in different amounts (25 to 300 mg) were added in 50 mL of 90 mg L⁻¹ Cr (VI) concentration solution at pH of 3. From Figure 3 (d) shows that CAB, the maximum Cr (VI) removal 35.12 % was achieved at 100 mg of adsorbent. The increasing dose up to 200 mg led to 52.19 % R of Cr (VI). The plausible explanation for this phenomenon is that, as the adsorbent dosage increases, the number of effective active sites and the available surface area for adsorption also increase⁽²³⁾. The increase in dose from 200 to 300 mg of adsorbent shows the negative result that reduce 2 % Cr (VI) removal, because with increasing adsorbent doses, limited Cr (VI) ions have the more adsorption space were available⁽²⁰⁾.

3.3 Potential applicability of CAB towards AMD

3.3.1 Effect of acidic ions on Cr (VI) removal efficiency

Figure 3 (e) illustrates the performance of the CAB beads in removing Cr (VI) in the presence of various ions typically found in acid drainage mines containing toxic heavy metals. To assess the impact of ionic strength on Cr (VI) adsorption, different acidic solutions (HCl, HNO₃, H₃PO₄, H₂SO₄) with concentrations of 1 mM and 25 mM of ionic solutions were employed. The results indicate that at higher ionic concentrations (25 mM), Cr (VI) removal decreases in H₂SO₄, HNO₃, and HCl, while it increases in H₃PO₄.

3.3.2 Reusability studies of CAB towards Cr (VI)

To assess the regenerative capability of the CAB adsorbents, 5 successive Adsorption-desorption experiments were conducted under optimized conditions, which is crucial for their repeated use in contaminant removal applications. The results depicted in Figure 3 (f), reveal that the Cr (VI) removal capacity decreased by 34.9% after the 5th cycle. Despite this reduction, the adsorption efficiency remained at 63.52 % after the 5th regeneration cycle, highlighting the favorable reusability of the adsorbent. Therefore, CAB can be readily employed for Cr (VI) adsorption, with NaOH treatment, for up to the 5th cycle. Furthermore, it exhibits a high desorption capacity, compared to previous study has shown ~ 60 % desorption⁽¹⁰⁾, while CAB shows nearly 98% desorption after each regeneration cycle, and only a marginal 2-3 % reduction in capacity. This suggests that it can be effectively used for the recovery of Cr (VI) ions from acid mine drainage (AMD).

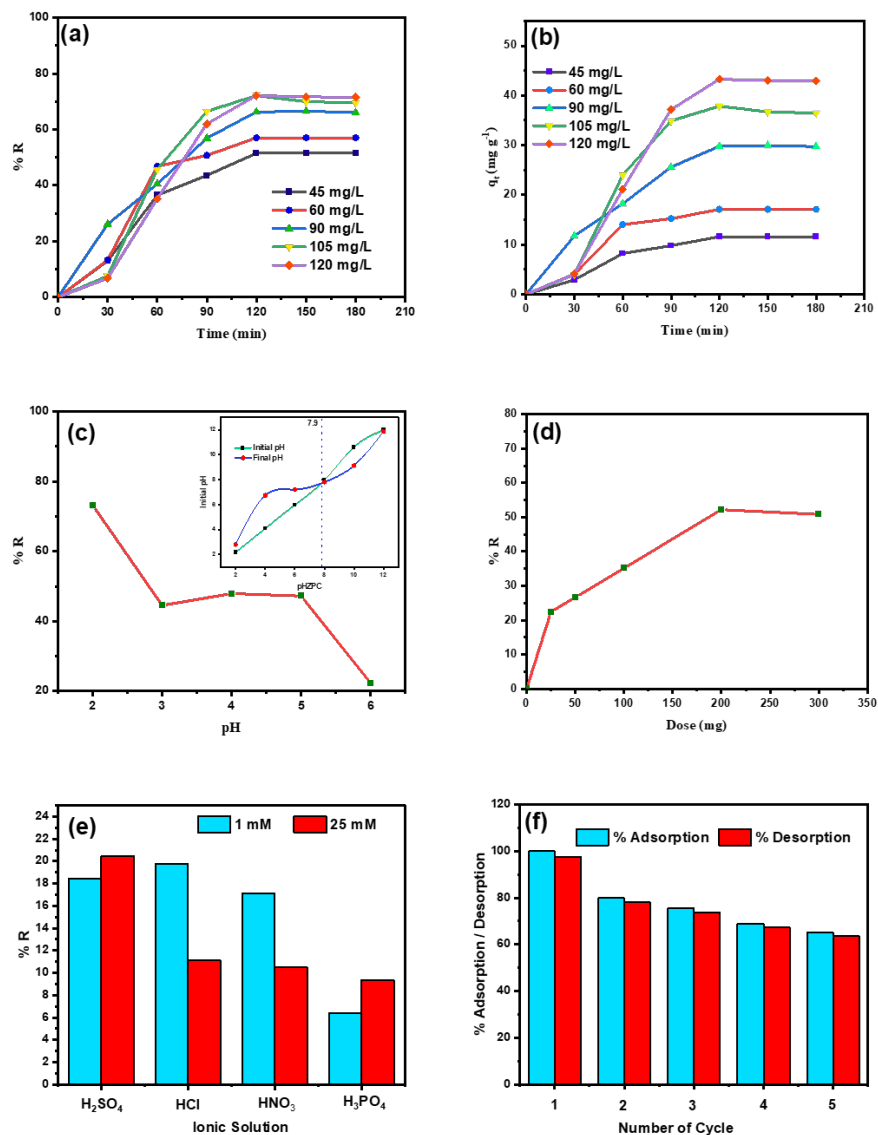


Fig 3. Optimization of the experimental parameters for the removal of Cr (VI) i.e., different concentrations and contact time using CAB % Removal (a) and q_e (mg g⁻¹) (b), effect of pH (c) and effect of adsorbent dose (d) and Ionic strength (e) and regeneration cycles study (f)

3.4 Cr (VI) adsorption isotherms and kinetics

The equilibrium adsorption data from the Cr (VI) adsorption studies were utilized to draw a plot at the equilibrium with various adsorbate concentration, as demonstrated in Figure 4 (a-c). This analysis was conducted to assess the applicability of three isotherm models: Langmuir, Freundlich, and Temkin, in representing the experimental data. The respective isotherm parameters and constants were determined, and their associated regression coefficient values (R^2) are detailed in Table 2. For the CAB adsorbent, the Langmuir isotherm model consistently yielded higher R^2 values, confirming its suitability for describing the experimental data.

Table 2. The Langmuir, Freundlich and Temkin isotherm parameters calculated for the adsorption of Cr (VI) on the surface of CAB

Isotherm Model	Isotherm Parameters	CAB
Langmuir Isotherm	q_m (mg g ⁻¹)	49.62
	k_L (L g ⁻¹)	0.08
	R^2	0.99
Freundlich isotherm	K_F (mg ^{1-1/n} L ^{1/n} g ⁻¹)	897.8
	n	0.334
	$1/n$	2.968
	R^2	0.993
Temkin isotherm	KT (L/mg)	0.0921
	BT J/mol	13.217
	R^2	0.9962

The Langmuir adsorption capacity (q_m) was 49.62 mg g⁻¹, indicating a substantial ability towards removal of Cr (VI). Furthermore, the values of the Freundlich constant (n) suggest that the adsorption of Cr (VI) onto CAB is primarily governed by physical adsorption processes. This result further less favorable to the Freundlich isotherm model in characterizing the adsorption behavior^(5,9,10).

To gain insights into the adsorption kinetics of Cr (VI) onto CAB, a range of kinetic rate models were employed, including the pseudo-first-order, pseudo-second order, and intraparticle diffusion models. The results derived from these models are illustrated in Figure 4(d-f), and the relevant parameters and rate constants are detailed in Table 3, along with their associated regression coefficient values (R^2). The findings indicate that both of the examined rate models exhibit good fits with the experimental data, emphasizing that the adsorption of Cr (VI) ions onto CAB is predominantly driven by physically mediated chemisorption. Importantly, for CAB, the pseudo-first-order model demonstrates a higher R^2 value. This finding suggests that the rate of change in solute uptake with time is directly proportional to the difference in saturation concentration and the amount of solid uptake over time. This model is typically applicable during the initial stage of an adsorption process⁽²⁴⁾. The Weber-Morris intraparticle diffusion model was utilized to clarify the diffusion mechanism of Cr (VI) ions onto CAB. The results, as depicted in Figure 4 (f), affirm a rapid single-phase sorption process for CAB. Nevertheless, this model doesn't discern between the transport phase and equilibrium phase, suggesting that the adsorbent may have vacant sites accessible for hosting the contaminant molecules. The computed intraparticle diffusion constants are furnished in Table 3. The comparison of maximum adsorption capacity of Cr (VI) and operational parameters of different adsorbents with CAB were listed in Table 4. The present study revealed that the microwave assisted synthesis of CAB provides facile synthesis in less time as well as better adsorption capacity with regeneration.

Table 3. The pseudo-first-order, pseudo-second-order and Intra-particle diffusion rate models calculated for the adsorption of on the surface of Cr (VI) on the surface of CAB

Kinetic models	Rate parameters for the adsorption Cr (VI)				
	C_0 (mg L ⁻¹)	$q_{e(exp)}$ (mg g ⁻¹)	k_1 (min ⁻¹)	$q_{e(cal)}$ (mg g ⁻¹)	R ²
Pseudo-first-order constants	45	11.5893	0.0219	13.2617	0.9658
	60	17.1074	0.0269	20.1141	0.9296
	90	29.7200	0.0212	32.8171	0.9579
	105	36.4700	0.0345	58.6408	0.8490
	120	42.8951	0.0221	57.5705	0.8508
Pseudo-second-order constants	C_0 (mg L ⁻¹)	$q_{e(exp)}$ (mg g ⁻¹)	k_2 (g mg ⁻¹ min ⁻¹)	$q_{e(cal)}$ (mg g ⁻¹)	R ²
	45	11.5893	0.0003	23.6407	0.6677
	60	17.1074	0.0002	35.4610	0.5288
	90	29.7200	0.0001	45.2489	0.9541
	105	36.4700	0.0001	45.2489	0.9541
Intraparticle Diffusion	C_0 (mg L ⁻¹)	$q_{e(exp)}$ (mg g ⁻¹)	K diff	C	R ²
	45	11.5893	0.9820	-0.3637	0.9308
	60	17.1074	1.4519	-0.2222	0.8910
	90	29.7200	2.4462	-0.0095	0.9649
	105	36.4700	3.2901	-3.0408	0.8606
120	42.8951	3.8640	-5.3810	0.8773	

Table 4. The comparison of maximum adsorption capacity of Cr (VI) and operational parameters of different adsorbents with CAB

Sr. No.	Adsorbent	pH	contact time (min)	Initial conc. (mg L ⁻¹)	Dose (g L ⁻¹)	Maximum adsorption capacity (mg g ⁻¹)	References
1.	Nano Water Treatment Residuals (nWTRs)	5	15	5 – 160	10	40.65	(1)
2.	Bulk Water Treatment Residuals (bWTRs)	5	15	5 – 160	10	2.78	(1)
3.	Natural zeolite	3	15	4.27	30	0.0262	(3)
4.	Ground Granulated Blast-Furnace Slag (GGBS)	3	15	4.27	150	0.0144	(3)
5.	SDS-chitosan beads	4	24 hours	10–6000	1	3.23	(5)
6.	Chitosan/Bentonite Composites (CSBT)	3	90	10	0.4	22.39	(10)
7.	Fe: Al: Pillared Bentonite (AIBT)	7	90	10	0.4	5.0	(10)
8.	chitosan/bentonite composite	3	210	50	10	5.0	(11)
9.	CAB	2	120	45-120	2	49.62	Present study

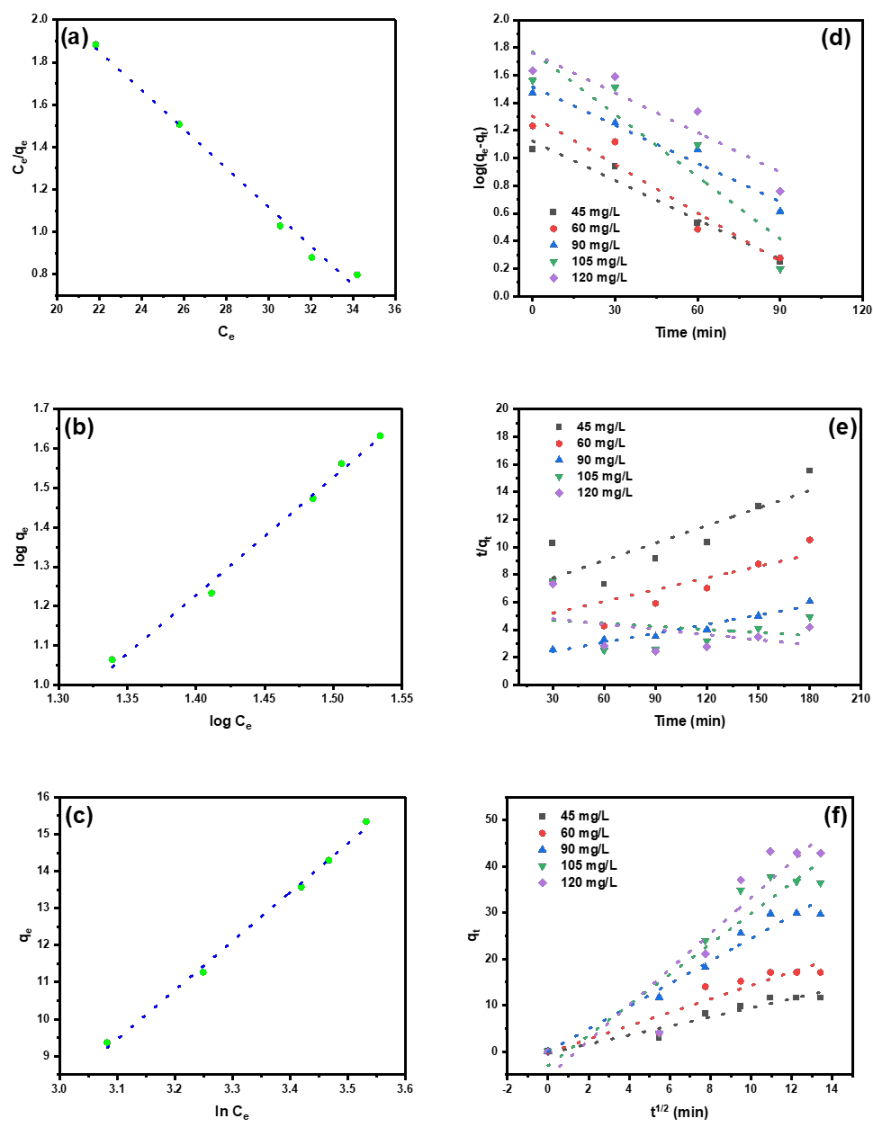


Fig 4. Isotherm modelling (Langmuir (a), Freundlich (b) and Temkin (c)), kinetic study (pseudo-first-order (d), pseudo-second-order (e) and Intraparticle diffusion model (f)) ($C_0 = 45$ to 120 mg L^{-1}) for the removal of Cr (VI) onto the synthesized adsorbent CAB

4 Conclusion

The microwave assisted low-cost adsorbent; Chitosan Activated Bentonite (CAB) nanocomposites were successfully synthesized for the removal of Chromium (Cr) from acidic environments. Comprehensive characterization was conducted, utilizing FTIR, XRD, and SEM-EDS analyses to examine the composition and surface morphology. The synthesized adsorbents were employed for the removal of Cr (VI) ions, with experiments exploring various parameters including initial concentration, contact time, dosage, and solution pH. Optimal removal efficiency, reaching 73.14%, was achieved at room temperature (27°C), a pH of 2, an initial concentration of 90 mg L^{-1} , and a dose of 2.0 g L^{-1} of CAB adsorbent. Field evaluations were conducted to assess field performance under varying acidic conditions and its regeneration capacity, revealing its potential for use in acid mine drainage (AMD) remediation. The kinetics models employed indicated pseudo-first-order behavior with better fitting R^2 value. The maximum adsorption capacity was found to be 49.62 mg g^{-1} , and the adsorption isotherm was well-fitted by the Langmuir model with best fitted R^2 value. The study demonstrates a low-cost adsorbent synthesis with novel method for CAB, which has a potential to removal of Cr (VI) from acid mine drainage as well as large scale production from the naturally available local

sources.

5 Acknowledgements

The present work is a part of the PhD thesis of Bharat V Thakcer, Reg. No. 159997106003. The authors would like to acknowledge Sophisticated Analytical Instrumentation Facility and Central Research Facilities at IIT-Bombay, Punjab University, SICART, V.V Nagar, Gujarat KSKV Kachchh University, Bhuj and GUIDE, Bhuj for providing research facilities for characterization and analysis of samples.

References

- 1) Wang H, Tan L, Hu B, Qiu M, Liang L, Bao L, et al. Removal of Cr(VI) from acid mine drainage with clay-biochar composite. *Desalination and Water Treatment*. 2019;165:212–221. Available from: <https://dx.doi.org/10.5004/dwt.2019.24572>.
- 2) Indian Minerals Yearbook 2020 (Part- III : MINERAL REVIEWS). 59th Edition. CHROMITE. 2022. Available from: https://ibm.gov.in/writereaddata/files/04272022163340Chromite_2020.pdf.
- 3) Shabalala AN, Basitere M. Interactive Relationship between Cementitious Materials and Acid Mine Drainage: Their Effects on Chromium Cr(VI) Removal. *Minerals*. 2020;10(11):1–17. Available from: <https://dx.doi.org/10.3390/min10110932>.
- 4) Islam MA, Angove MJ, Morton DW. Recent innovative research on chromium (VI) adsorption mechanism. *Environmental Nanotechnology, Monitoring & Management*. 2019;12. Available from: <https://dx.doi.org/10.1016/j.enmm.2019.100267>.
- 5) Du X, Kishima C, Zhang H, Miyamoto N, Kano N. Removal of Chromium(VI) by Chitosan Beads Modified with Sodium Dodecyl Sulfate (SDS). *Applied Sciences*. 2020;10(14):1–23. Available from: <https://dx.doi.org/10.3390/app10144745>.
- 6) Liu Y, Jia J, Zhang H, Sun S. Enhanced Cr(VI) stabilization in soil by chitosan/bentonite composites. *Ecotoxicology and Environmental Safety*. 2022;238:1–7. Available from: <https://dx.doi.org/10.1016/j.ecoenv.2022.113573>.
- 7) Xu X, Cheng Y, Wu X, Fan P, Song R. La(III)-bentonite/chitosan composite: A new type adsorbent for rapid removal of phosphate from water bodies. *Applied Clay Science*. 2020;190. Available from: <https://dx.doi.org/10.1016/j.clay.2020.105547>.
- 8) Biswas S, Fatema J, Debnath T, Rashid TU. Chitosan–Clay Composites for Wastewater Treatment: A State-of-the-Art Review. *ACS ES&T Water*. 2021;1(5):1055–1085. Available from: <https://dx.doi.org/10.1021/acsestwater.0c00207>.
- 9) Majiya H, Clegg F, Sammon C. Bentonite-Chitosan composites or beads for lead (Pb) adsorption: Design, preparation, and characterisation. *Applied Clay Science*. 2023;246:1–15. Available from: <https://dx.doi.org/10.1016/j.clay.2023.107180>.
- 10) Jia J, Liu Y, Sun S. Preparation and Characterization of Chitosan/Bentonite Composites for Cr (VI) Removal from Aqueous Solutions. *Adsorption Science & Technology*. 2021;2021:1–15. Available from: <https://dx.doi.org/10.1155/2021/6681486>.
- 11) Yang J, Huang B, Lin M. Adsorption of Hexavalent Chromium from Aqueous Solution by a Chitosan/Bentonite Composite: Isotherm, Kinetics, and Thermodynamics Studies. *Journal of Chemical & Engineering Data*. 2020;65(5):2751–2763. Available from: <https://dx.doi.org/10.1021/acs.jced.0c00085>.
- 12) Shabanzade H, Salem A, Salem S. Efficient removal of contaminants from waste lubricant oil by nano-porous bentonite produced via microwave-assisted rapid activation: process identifications and optimization. *Environmental Science and Pollution Research*. 2019;26(23):23257–23267. Available from: <https://dx.doi.org/10.1007/s11356-019-05625-w>.
- 13) Priyadarshi G, Raval NP, Trivedi MH. Microwave-assisted synthesis of cross-linked chitosan-metal oxide nanocomposite for methyl orange dye removal from unary and complex effluent matrices. *International Journal of Biological Macromolecules*. 2022;219:53–67. Available from: <https://dx.doi.org/10.1016/j.ijbiomac.2022.07.239>.
- 14) Raval NP, Priyadarshi GV, Mukherjee S, Zala H, Fatma D, Bonilla-Petriciolet A, et al. Statistical physics modeling and evaluation of adsorption properties of chitosan-zinc oxide nanocomposites for the removal of an anionic dye. *Journal of Environmental Chemical Engineering*. 2022;10(6). Available from: <https://dx.doi.org/10.1016/j.jece.2022.108873>.
- 15) Thacker BV, Vadodaria GP, Priyadarshi GV, Trivedi MH. Biopolymer-based fly ash-activated zeolite for the removal of chromium from acid mine drainage. *The Scientific Temper*. 2023;14(04):1217–1226. Available from: <https://dx.doi.org/10.58414/scientifictemper.2023.14.4.24>.
- 16) Al-Maliky EA, Gzar HA, Al-Azawy MG. Determination of Point of Zero Charge (PZC) of Concrete Particles Adsorbents. In: The 1st International Conference on Advanced Research in Engineering Sciences and Technology (ICAREST 2021) ;vol. 1184 of IOP Conference Series: Materials Science and Engineering. IOP Publishing. 2021;p. 1–8. Available from: <https://dx.doi.org/10.1088/1757-899x/1184/1/012004>.
- 17) Yang J, Huang B, Lin M. Adsorption of Hexavalent Chromium from Aqueous Solution by a Chitosan/Bentonite Composite: Isotherm, Kinetics, and Thermodynamics Studies. *Journal of Chemical & Engineering Data*. 2020;65(5):2751–2763. Available from: <https://dx.doi.org/10.1021/acs.jced.0c00085>.
- 18) da Silva JCS, França DB, Rodrigues F, Oliveira DM, Trigueiro P, Filho ECS, et al. What happens when chitosan meets bentonite under microwave-assisted conditions? Clay-based hybrid nanocomposites for dye adsorption. *Colloids and Surfaces A: Physicochemical and Engineering Aspects*. 2021;609. Available from: <https://dx.doi.org/10.1016/j.colsurfa.2020.125584>.
- 19) Hidayat E, Yoshino T, Yonemura S, Mitoma Y, Harada H. A Carbonized Zeolite/Chitosan Composite as an Adsorbent for Copper (II) and Chromium (VI) Removal from Water. *Materials*. 2023;16(6):1–13. Available from: <https://dx.doi.org/10.3390/ma16062532>.
- 20) Zhang S, Zhang Y, Fu L, Jing M. A chitosan fiber as green material for removing Cr(VI) ions and Cu(II) ions pollutants. *Scientific Reports*. 2021;11(1):1–9. Available from: <https://dx.doi.org/10.1038/s41598-021-02399-5>.
- 21) Yuan X, Li J, Luo L, Zhong Z, Xie X. Advances in Sorptive Removal of Hexavalent Chromium (Cr(VI)) in Aqueous Solutions Using Polymeric Materials. *Polymers*. 2023;15(2):1–34. Available from: <https://dx.doi.org/10.3390/polym15020388>.
- 22) Altun T. Preparation and application of glutaraldehyde cross-linked chitosan coated bentonite clay capsules: chromium(VI) removal from aqueous solution. *Journal of the Chilean Chemical Society*. 2020;65(2):4790–4797. Available from: <https://www.scielo.cl/pdf/jcchems/v65n2/0717-9707-jcchems-65-02-4790.pdf>.
- 23) Hamadeen HM, Elkhatib EA, Moharem ML. Optimization and mechanisms of rapid adsorptive removal of chromium (VI) from wastewater using industrial waste derived nanoparticles. *Scientific Reports*. 2022;12(1):1–12. Available from: <https://dx.doi.org/10.1038/s41598-022-18494-0>.
- 24) Krstić V. Role of zeolite adsorbent in water treatment. In: Handbook of Nanomaterials for Wastewater Treatment. Elsevier. 2021;p. 417–481. Available from: <https://doi.org/10.1016/B978-0-12-821496-1.00024-6>.